Magnetic response in the underdoped cuprates

A. J. A. James, R. M. Konik, and T. M. Rice

Phys. Rev. B **86**, 100508 — Published 25 September 2012

DOI: 10.1103/PhysRevB.86.100508

Magnetic Response in the Underdoped Cuprates

A. J. A. James,[1] R. M. Konik,[1] and T. M. Rice[1,2]

[1] *Condensed Matter Physics and Material Science Department, Brookhaven National Laboratory, Upton, NY 11973*

[2] *Institut für Theoretische Physik, ETH Zürich, CH-8093, Zürich, Switzerland*

We examine the dynamical magnetic response of the underdoped cuprates by employing a phenomenological theory of a doped resonant valence bond state where the Fermi surface is truncated into four pockets. This theory predicts a resonant spin response which with increasing energy (0 to 100meV) appears as an hourglass. The very low energy spin response is found at $(\pi, \pi \pm \delta)$ and $(\pi \pm \delta, \pi)$ and is determined by scattering from the pockets' frontside to the tips of opposite pockets where a van Hove singularity resides. At energies beyond 100 meV, strong scattering is seen from $(\pi, 0)$ to (π, π). This theory thus provides a semi-quantitative description of the spin response seen in both INS and RIXS experiments at all relevant energy scales.

PACS numbers: 74.25.Ha,74.20.Mn,74.72.Gh

Introduction: Neutron scattering studies of the magnetic properties of underdoped cuprate superconductors have revealed an unusual 'hourglass' pattern in the spin excitation spectrum that persists into the normal state [1]. This spectrum, centered on (π, π), can be divided into three energy regions. At low energies the weight is shifted to nearby incommensurate wavevectors, peaking along the crystal axes. With increasing energy the weight moves towards (π, π) and is more uniformly distributed about this wavevector. Whether this inward dispersion reaches (π, π) depends on the particular cuprate being examined. At still higher energies a uniform ring appears evolving away from (π, π). Recent RIXS experiments [2] have explored this high energy region further.

A phenomenological theory for the underdoped pseudogap phase by Yang, Rice and Zhang (YRZ) [3] has had considerable success in reproducing many electronic quasi-particle properties [4], both in STM [5] and in ARPES [6] experiments. Heretofore, a prediction of the spin response based on this phenomenology has not been developed. In part this is because YRZ was developed as a phenomenological ansatz for the single particle Green's function (GF) [3] and it was unclear how to extend it to the spin response, $S(\omega, k)$. In this letter we present a derivation of YRZ from a microscopic model and then use a consistent set of microscopics to calculate $S(\omega, k)$. We show that this $S(\omega, k)$ reproduces key features of the experiments just described, at all three energy scales, in particular recent RIXS experiments [2]. We thus demonstrate that the YRZ phenomenology can provide a consistent description for a wide range of phenomena and energies in the underdoped cuprates.

In doing so, this work entangles itself in the intensely debated question of whether the magnetic response in the cuprates arises from itinerant electrons or from localized electrons [7, 8]. While we argue that the magnetic response can be explained by itinerant electrons (the YRZ quasiparticles), an important body of work [9, 10] associates this magnetic phenomena with spin and charge density waves (i.e. stripes) which appear as incommensurate quasi-elastic peaks in the magnetic response. While we cannot decide this argument, we demonstrate that it is possible at least for an itinerant picture to describe phenomena such as the low energy hourglass that appears naturally in the stripe picture.

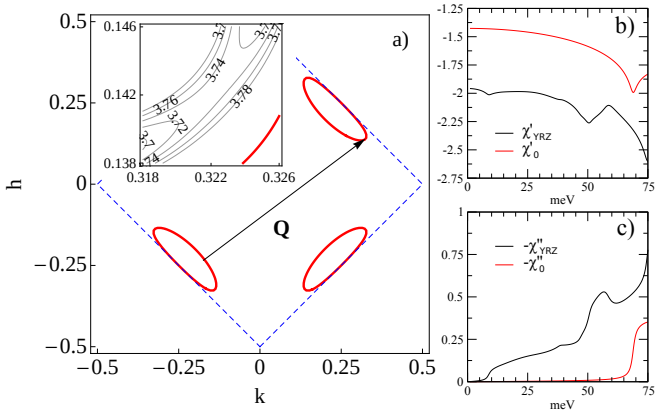

FIG. 1: a) The Fermi surface for hole doping, $x = 0.12$. Hole pockets are marked in red (solid) while the lines of Luttinger zeros are blue (dashed). Also marked is a nesting vector $\mathbf{Q} = (0.5, 0.375)$ (in reciprocal lattice units), connecting the tip of a pocket to the frontside of another pocket. Inset: At the tip of the pocket there is a saddlepoint in the superconducting quasi-particle dispersion and hence a van Hove singularity. Energy contours are labelled in meV. The parameters used here are $t(x) = 70$meV, $t'(x) = -0.18t(x)$, $t''(x) = 0.12t(x)$, $\Delta_0 = 0.34t(x)$ and $\Delta_{SC} = 0.05t(x)$. b) The real parts of $\chi_{YRZ}(\omega, \mathbf{Q})$ and $\chi_0(\omega, \mathbf{Q})$ vs. ω. c) The imaginary parts.

YRZ Spin Response: The YRZ ansatz, as originally conceived, was for the single particle GF of the underdoped cuprates. The associated Fermi surface is truncated and composed of four nodal pockets (Fig. 1) with area proportional to the doping, x. This GF is also characterized by lines of Luttinger zeros which coincide with the magnetic Brillouin zone (BZ) or Umklapp sur-

face [12] (see Fig. 1). The ansatz was inspired by an analysis of a system of weakly coupled Hubbard ladders where a similar phenomenology was found [13].

To extend the YRZ ansatz to the spin response, we first elucidate the connection between YRZ and the slave boson (SB) treatment of the t-J Hamiltonian. SBs provide a natural RPA-like form for the spin response and we intend to adapt this to the assumptions of YRZ. In this way we will arrive at a form for the spin response that takes into account the same assumptions used in the YRZ form of the single particle GF. We write the $t-J$ Hamiltonian as

$$\begin{aligned} H &= -\sum_{ij\sigma} t_{ij}^{nn} c_{i\sigma}^\dagger c_{j\sigma} - \sum_{ij\sigma} t_{ij}^{nnn} c_{i\sigma}^\dagger c_{j\sigma} + \frac{1}{2}\sum_{ij} J_H S_i \cdot S_j \\ &\equiv H_t^{nn} + H_t^{nnn} + H_{J_H} \end{aligned} \tag{1}$$

The Hamiltonian is divided into terms involving nearest neighbour (NN) hopping, H_t^{nn}, next nearest neighbour (NNN) hopping (and beyond), H_t^{nnn}, and a spin-spin interaction, H_{J_H}. We now subject $H_t^{nn} + H_{J_H}$ to the standard slave boson mean field theory (SBMFT) treatment (leaving H_t^{nnn} to later). We thus factor the fermions, $c_{i\sigma}^\dagger$, into spinons, $f_{i\sigma}^\dagger$ and holons, b_i via $c_{i\sigma}^\dagger = f_{i\sigma}^\dagger b_i$, where the spinons and holons are subject to the constraint $\sum_\sigma f_{i\sigma}^\dagger f_{i\sigma} + b_i^\dagger b_i = 1$. At this level the spinon GF is [14]

$$G_\sigma^f(\omega, \mathbf{k}) = \frac{1}{\omega - \xi_0(\mathbf{k}) - \Sigma_R(\omega, \mathbf{k})}, \tag{2}$$

where $\Sigma_R = |\Delta_R(\mathbf{k})|^2/(\omega + \xi_0(\mathbf{k}))$ and $\Delta_R(\mathbf{k}) = \Delta_0(x)(\cos k_x - \cos k_y)$. Here $t(x)$ and $\Delta_0(x)$ are doping dependent parameters. The single particle GF, G_σ^c, is given directly in terms of the spinon GF because we assume the bosons are nearly condensed, replacing the boson propagator $\langle b_i^\dagger(\tau) b_j(0)\rangle$ by $g_t(x)$: $G_\sigma^c(\omega, \mathbf{k}) = g_t(x) G_\sigma^f(\omega, \mathbf{k})$ (in SBMFT $g_t(x) = x$ [14]; in the Gutzwiller approximation $g_t(x) = 2x/(1+x)$ [3]). This differs from the YRZ form in that the full dispersion in the denominator is replaced by the dispersion due to NN hopping.

Following a recent suggestion by P. A. Lee [11], we bridge the gap between the SBMFT and YRZ, by returning to the neglected NNN hopping, H_t^{nnn}. Treating this term in mean field theory (MFT) moves the Luttinger zeros off the magnetic Brillouin zone and so we instead use an RPA like approximation (Fig. 2) leading to

$$G_\sigma^f(\omega, \mathbf{k}) = \frac{1}{\omega - \xi_0(\mathbf{k}) - \xi'(\mathbf{k}) - \Sigma_R(\omega, \mathbf{k})}. \tag{3}$$

Here $\xi'(k) = -4t'(x)\cos k_x \cos k_y - 2t''(x)(\cos 2k_x + \cos 2k_y)$ is the dispersion due to the NNN terms. The spinon propagator in this form now gives the YRZ ansatz. The key consequence of the non-MFT treatment of the

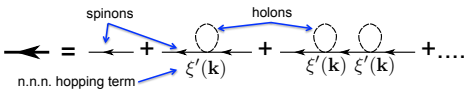

FIG. 2: RPA form of the YRZ spinon propagator in terms of SB propagators.

H_t^{nnn} and a central feature of our phenomenology is that spinons and holons are bound together. This binding distinguishes YRZ from the standard SBMFT approximation which produces an expanded Hilbert space with independent spinons and holons. Lest this distinction between H_t^{nnn} and H_t^{nn} seem artificial, we derive in Ref. 15 a YRZ-like ansatz for $G_\sigma^f(\omega, k)$ by treating H_t^{nn} and H_t^{nnn} on the same footing, i.e. both as the glue binding spinons to holons. This $G_\sigma^f(\omega, k)$ differs only slightly in the values of its various coefficients. Here however, we make the distinction above to keep to the original YRZ conventions of Ref. 3.

A second consequence is the absence of an anomalous spinon propagator (or at least its coherent part), consistent with an underlying assumption that spin correlations are only short-ranged in the YRZ ansatz. This form (Eqn. 3) applies in the normal phase and can be generalized to the d-wave superconducting state, e.g. see [4]. Note that YRZ gives a two-gap description of the pseudogap phase with separate RVB (Δ_0) and pairing Δ_{SC} gaps.

We now turn to the spin response: in SBMFT, neglecting the effects of spinon–holon binding, this naturally takes on an RPA-like form [14]:

$$S(\omega, \mathbf{k}) = -\frac{3}{\pi}\mathrm{Im}\frac{\chi_0(\omega, \mathbf{k})}{1 - J(\mathbf{k})\chi_0(\omega, \mathbf{k})}. \tag{4}$$

Here $\chi_0(\omega, \mathbf{k})$ is the bare particle-hole bubble for the spinons (including anomalous contributions) and $J(\mathbf{k}) = J(\cos k_x + \cos k_y)$.

How now does our non-mean field treatment of H_t^{nnn} alter this? Firstly we no longer include a contribution to χ_0 from the anomalous spinon GF. And to determine how t^{nnn} dresses the normal spinon Green's functions, we employ the same approximation that led to the YRZ ansatz. This means the derivation of both $G_\sigma^f(\omega, k)$ and $S_{YRZ}(\omega, k)$ are self-consistent. Namely we only allow diagrams involving vertices where the boson lines of the vertex are tied together. With this restriction, t^{nnn} only dresses the individual spinon propagators making up the particle-hole bubble entering χ_0. The YRZ spin response is then

$$S_{YRZ}(\omega, \mathbf{k}) = -\frac{3}{\pi}\mathrm{Im}\frac{\chi_{YRZ}(\omega, \mathbf{k})}{1 - J(\mathbf{k})\chi_{YRZ}(\omega, \mathbf{k})}, \tag{5}$$

where χ_{YRZ} is simply a particle-hole bubble of YRZ quasi-particles.

In computing $S_{YRZ}(\omega, \mathbf{k})$ we treat J as a fitting parameter for each doping, different from J_H. We do not expect the underlying mean field treatment to accurately treat the renormalization of J which is inevitably doping dependent. In particular in the presence of strong scattering connecting the magnetic Brillouin zone boundaries, we expect J to be strongly modified. This is not merely a feature of YRZ but is generic to slave boson flavored theories: in Ref. [14], J had to be sharply reduced to produce an ordering transition at approximately the correct doping.

Results: We begin with the lower energy ($\omega < 100$meV) spin response in the underdoped cuprates which has a universal hour glass shape [1, 16–18] as described in the introduction, with strong incommensurate response at low energies (i.e. $\omega \approx 2\Delta_{SC}$) concentrated at four points, $(\pi, \pi \pm \delta)$ and $(\pi \pm \delta, \pi)$.

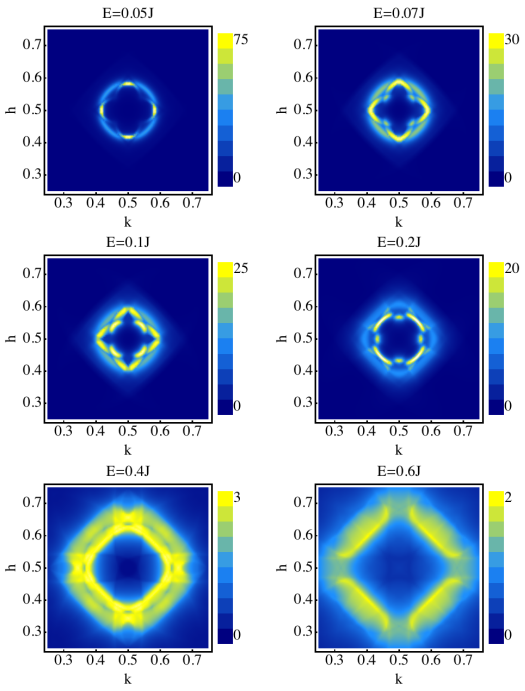

FIG. 3: Constant energy slices of the spin response for $x = 0.12$ in the SC phase – the parameters used are the same as listed in Fig. 1, with $J = 140$meV for our theory.

We see these general features in constant energy scans of $S_{YRZ}(\omega, \mathbf{k})$ as presented in Fig. 3 for the superconducting case. In this figure we have chosen parameters appropriate for the description of underdoped $La_{2-x}Sr_xCuO_4$. At very low energies ($0.05J$) the primary response is at $(\pi, \pi \pm \delta)$ and $(\pi \pm \delta, \pi)$ with $\delta = 0.16\pi$. As the energy increases there is a slight inward dispersion (δ decreases slightly) albeit in an uneven fashion (there is a sudden movement inward at $0.125J$) with the response simultaneously becoming more isotropic (circular) about (π, π). This dispersion reverses at $\omega \sim 0.2J$ and begins to move outwards. In this energy range the greatest response is found about $(\pi \pm \delta', \pi \pm \delta')$. The behavior is consistent with underdoped and optimally doped $La_{2-x}Sr_xCuO_4$ [16–18]. It is also seen in stripe stabilized $La_{2-x}Ba_xCuO_4$ [20] and YBCO [1, 19]. We explicitly plot in Fig. 4a the $\mathbf{k}$-point of maximal intensity as a function of energy, comparing it with a number of cuprates.

The response found at $(\pi, \pi \pm \delta)$ and $(\pi \pm \delta, \pi)$ at $0.05J$meV can be directly ascribed to transitions between the fronts of the pockets and the tips of opposite pockets (the vector Q in Fig. 1). In general the presence of the pockets in the YRZ theory allows for low energy scattering in a larger portion of the Brillouin zone than in theories where the spinon Fermi surface consists of four points coinciding with nodes of the SC order parameter (see Figs. 1b and 1c for a comparison of χ_{YRZ} and χ_0; χ_0 is the bare particle-hole bubble for the standard slave boson description of the spin response [14]). Moreover in the presence of a SC gap, the tips of the pockets see a saddle point in dispersion with a corresponding van Hove singularity further enhancing the low energy scattering.

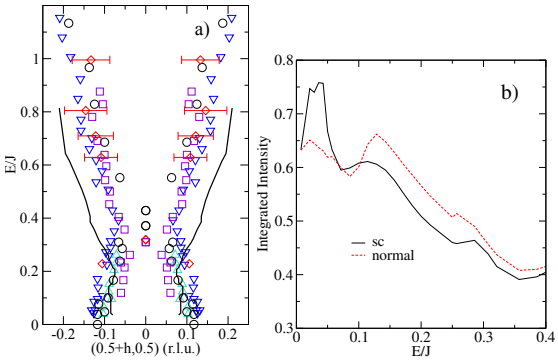

FIG. 4: a) Hourglass dispersion of the resonance near π, π. The thick black line is the position of the maximum intensity peak after integrating the numerical data over a strip of width $2\pi/25$ along the parallel direction, averaged over sections of length $2\pi/33$. Experimental data points (appropriately rescaled) are taken from [1, 19]: 'up' triangles, $La_{1.90}Sr_{0.10}CuO_4$ [16]; circles, $La_{1.875}Ba_{0.125}CuO_4$ [20]; 'down' triangles, $La_{1.84}Sr_{0.16}CuO_4$ [18]; squares, $YBa_2Cu_3O_{6.5}$ [21] and diamonds, $YBa_2Cu_3O_{6.6}$ [22]. b) k-integrated spin response with and without a superconducting gap.

In the normal state, low energy spectral weight is found not just in directions parallel to the crystal axes but in the nodal directions as well (see Fig. 5). This is a result of the disappearance of the saddlepoint identified in Fig. 1 in the normal state. While parallel scattering still dominates at low energies, the response is less concentrated in such areas and weight does appear along the nodal directions (at least in the LSCO family) [16, 17].

Underlying our calculations of the magnetic response is the assumption that itinerant quasi-particles (even if heavily dressed) can explain this response in the cuprates.

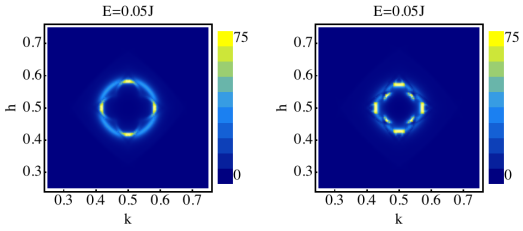

FIG. 5: $x = 0.12$ and $\omega = 0.05$J constant energy slices for the SC phase (left) and the normal phase (right).

While there is evidence that at least part of the spin response must be ascribed to localized spins [7, 20], there is also evidence that impurities introduce local spins, e.g. Zn doped into YBCO [23] and earlier studies. The full cuprate magnetic response requires a mixture of the two. However one experimental feature of the spin response that points to itinerant quasi-particles is the depression of the **k**-integrated spin response at $\omega < 2\Delta_{SC}$ upon decreasing $T < T_c$. This behavior is seen in both the LSCO [16–18] and YBCO [24] families and we see it as well in our calculations (Fig. 4b). We also see in Fig. 4b that our calculated integrated intensity has a two peak structure, with one peak at energies close to $0.05J$ and one at energies at $\approx 0.12J$. This doubling of peaks is seen in near optimally doped LSCO [17, 18]. In underdoped LSCO at least the lower energy peak has been observed [16].

Turning to high energies, $\omega > 100$meV, we find the YRZ spin response is able to explain key features in the spin response recently measured by RIXS. In Fig. 6 we plot the spin response for energies 100meV $< \omega <$ 300meV for two cuts in the Brillouin zone. We see two features emanating from $(0, 0)$. One disperses towards $(\pi, 0)$ as energy is increased (corresponding well with the reported paramagnon-like excitation in the RIXS data of [2] on a variety of cuprates). The other, with a considerably greater spin velocity, evolves towards (π, π). This dispersing paramagnon excitation naturally appears from a two-band factorization of YRZ (an exact rewriting of Eqn. 3) [4]:

$$G^f_\sigma(\omega, \mathbf{k}) = \frac{z_+(\mathbf{k})}{\omega - \omega_+(\mathbf{k})} + \frac{z_-(\mathbf{k})}{\omega - \omega_-(\mathbf{k})}. \qquad (6)$$

The paramagnon results from a particle-hole excitation from the lower band, $\omega_-(\mathbf{k})$, to the upper band, $\omega_+(\mathbf{k})$. This feature is particularly robust as it only relies on the factorization of YRZ into two effective bands. Note that the low energy response is primarily due to intraband transitions within the lower, $\omega_-(\mathbf{k})$, band.

In conclusion we have shown that calculations of the magnetic response based upon itinerant YRZ quasiparticles satisfactorily reproduce key features of experiments on the spin response of the underdoped cuprates at both low and high energies.

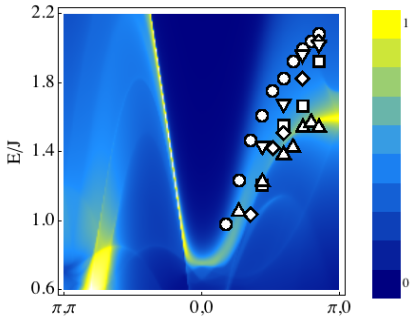

FIG. 6: The spin response for energies from 100meV to 300meV, for cuts from (π, π) to $(0, 0)$ to $(\pi, 0)$ in the Brillouin zone (same choice of parameters as previously). Also plotted are data points from [2]: circles, $Nd_{1.2}Ba_{1.8}Cu_3O_6$; squares, $YBa_2Cu_3O_7$; diamonds, $Nd_{1.2}Ba_{1.8}Cu_3O_7$; 'up' triangles, $YBa_2Cu_4O_8$; 'down' triangles, $YBa_2Cu_3O_{6.6}$. Here $J = 140$meV.

The authors acknowledge support from the Center for Emergent Superconductivity, an Energy Frontier Research Center funded by the DOE Office of Science, Office of Basic Energy Science under award DE-AC0298CH1088. TMR also acknowledges support from the Swiss National Science Foundation. We also thank J. Tranquada, J. Hill, and M. Dean for useful conversations.

[1] For a recent review see M. Fujita et al., J. Phys. Soc. Jpn. (in press); arXiv:1108.4431.
[2] M. Le Tacon et al., Nature Physics **7**, 725 (2011).
[3] K.-Y. Yang, T. M. Rice, and F.-C. Zhang, Phys. Rev. B **73**, 174501 (2006).
[4] T. M. Rice, K.-Y. Yang, and F.-C. Zhang, Rep. Prog. Phys. **75**, 01650 (2012).
[5] A. R. Schmidt et al., New J. Phys. **13**, 065014 (2011); Y. Kohsaka et al., Nature **454**, 1072 (2008).
[6] H.-B. Yang et al, Phys. Rev. Lett. **107**, 047003 (2011).
[7] Xu et al., Nature Physics **5**, 642 (2009).
[8] M. Vojta, Nature Physics **5**, 623 (2009); ibid. Nature Physics **7**, 674 (2011).
[9] G.S. Uhrig et al., J. Phys. Soc. Jpn. **74** Supplement 86 (2005).
[10] M. Vojta, Adv. in Phys. **58** 699 (2009).
[11] Private communication from P. A. Lee. P.A. Lee's suggestion is in turn based on T.K. Ng, Phys. Rev. B **71**, 172509 (2005).
[12] C. Honerkamp et al., Phys. Rev. B **63**, 035109 (2001).
[13] R. M. Konik, T. M. Rice, and A. Tsvelik, Phys. Rev. Lett. **96**, 086407 (2006).
[14] J. Brinckmann and P. A. Lee, Phys. Rev. B **65**, 014502 (2001).
[15] See supplementary material.
[16] O. J. Lipscombe, B. Vignolle, T. G. Perring, C. D. Frost, and S. M. Hayden, Phys. Rev. Lett. **102**, 167002 (2009).
[17] N. B. Christensen et al., Phys. Rev. Lett. **93**, 147002 (2004).
[18] B. Vignolle, et al., Nature Physics **3**, 163 (2007).
[19] J. Tranquada, chapter in Handbook of High-Temperature Superconductivity: Theory and Experiment, ed. J. R. Schrieffer, Springer (2007).
[20] J. M. Tranquada et al., Nature **429**, 534 (2004).
[21] C. Stock et al., Phys. Rev. B **71**, 024522 (2005).
[22] S. M. Hayden et al., Nature **429**, 531 (2004).
[23] A. Suchaneck et al., Phys. Rev. Lett. **105**, 037207 (2010).
[24] C. Stock et al., Phys. Rev. B **69**, 014502, (2004).